Published in final edited form as:
Cell. 2014 October 9; 159(2): 267–280. doi:10.1016/j.cell.2014.09.011.

Chemosensation of Bacterial Secondary Metabolites Modulates Neuroendocrine Signaling and Behavior of *C. elegans*

Joshua D. Meisel[1], **Oishika Panda**[2], **Parag Mahanti**[2], **Frank C. Schroeder**[2], and **Dennis H. Kim**[1,*]

[1]Department of Biology, Massachusetts Institute of Technology, Cambridge, MA 02139 USA

[2]Boyce Thompson Institute and Department of Chemistry and Chemical Biology, Cornell University, Ithaca, NY 14853 USA

Summary

Discrimination among pathogenic and beneficial microbes is essential for host organism immunity and homeostasis. Here, we show that chemosensory detection of two secondary metabolites produced by *Pseudomonas aeruginosa* modulates a neuroendocrine signaling pathway that promotes avoidance behavior in the simple animal host *Caenorhabditis elegans*. Secondary metabolites phenazine-1-carboxamide and pyochelin activate a G protein-signaling pathway in the ASJ chemosensory neuron pair that induces expression of the neuromodulator DAF-7/TGF-β. DAF-7, in turn, activates a canonical TGF-β signaling pathway in adjacent interneurons to modulate aerotaxis behavior and promote avoidance of pathogenic *P. aeruginosa*. Our data provide a chemical, genetic, and neuronal basis for how the behavior and physiology of a simple animal host can be modified by the microbial environment, and suggest that secondary metabolites produced by microbes may provide environmental cues that contribute to pathogen recognition and host survival.

Keywords

host-microbe interactions; *Caenorhabditis elegans*; *Pseudomonas aeruginosa*; TGF-β signaling; neuropeptides; pathogen avoidance behavior; bacterial secondary metabolites

Introduction

The recognition of microbial pathogens and the corresponding danger they represent is essential for the survival of host organisms. Innate immune systems have evolved to respond

*Correspondence to: dhkim@mit.edu.

Author Contributions

J.D.M. performed *C. elegans* and *P. aeruginosa* experiments. O.P. and P.M. performed fractionation and NMR analysis. J.D.M., O.P., F.C.S., and D.H.K, analyzed the data and interpreted results. J.D.M. and D.H.K. wrote the paper with input from O.P. and F.C.S.

to foreign structures derived from microbes, which help the host distinguish microbes from self. However, such molecular patterns do not necessarily help the host discriminate a microbe that is pathogenic from one that is commensal. Microbial molecular patterns such as lipopolysaccharide are found on pathogen and commensal alike. In view of the diversity of olfactory receptors present even in relatively simple host organisms, chemosensory responses offer the potential to detect a far greater set of relevant microbial molecules. Candidate receptors and specific bacterial cues that modulate host physiology and avoidance behavior have begun to be explored (Pradel et al., 2007; Rivière et al., 2009; Stensmyr et al., 2012).

The soil dwelling nematode *Caenorhabditis elegans* is a simple host organism that forages on decomposing organic matter for bacterial food (Félix and Duveau, 2012). The presence of bacterial food affects diverse behaviors of *C. elegans* such as feeding, locomotion, thermotaxis, and aerotaxis (Avery and Horvitz, 1990; Chang et al., 2006; Hedgecock and Russell, 1975; Sawin et al., 2000), and differences in the species composition of the food supply can alter aspects of their physiology and behavior (Gusarov et al., 2013; MacNeil et al., 2013; Shtonda and Avery, 2006; Watson et al., 2014). Pathogenic bacteria kill *C. elegans* and induce an aversive learning response (Zhang et al., 2005) that promotes protective behavioral avoidance (Chang et al., 2011; Pradel et al., 2007; Pujol et al., 2001; Reddy et al., 2009). Bacterial molecules including *Serratia marcescens* serrawettin and *Pseudomonas aeruginosa* quorum-sensing regulators have been implicated in the behavioral avoidance of bacterial lawns (Beale et al., 2006; Pradel et al., 2007). As such, *C. elegans* is emerging as a useful model for dissecting the genetic and biochemical mechanisms underlying microbial discrimination in animal hosts.

In this study we focus on how the DAF-7/TGF-β pathway functions in chemosensory neurons of *C. elegans* to regulate behavior in response to changes in the microbial environment. DAF-7 functions in the neuroendocrine regulation of diverse aspects of organismal development and physiology, including the dauer developmental decision, foraging and aggregation behaviors, quiescence, metabolism, and longevity (de Bono et al., 2002; Gallagher et al., 2013; Greer et al., 2008; Milward et al., 2011; Shaw et al., 2007; Swanson and Riddle, 1981). In addition, another *C. elegans* TGF-β-family ligand, DBL-1, has been shown to regulate olfactory aversive learning and antifungal defenses (Zhang and Zhang, 2012; Zugasti and Ewbank, 2009). Expression of *daf-7* is limited to the ASI pair of chemosensory neurons and has been shown to respond to the availability of bacterial food (Ren et al., 1996; Schackwitz et al., 1996). Here, we show that chemosensory recognition of the pathogenic bacterium *P. aeruginosa* dramatically alters the neuronal expression pattern of DAF-7 to promote avoidance behavior. Through a forward genetic screen we identify conserved components of G protein signaling that act cell-autonomously in the ASJ neurons to activate transcription of *daf-7* in response to *P. aeruginosa*. Finally, we show that the ASJ neurons respond to the secondary metabolites phenazine-1-carboxamide and pyochelin secreted by *P. aeruginosa* during stationary phase. Our findings demonstrate how specific bacteria can exert effects on host behavior and physiology, and point to how secondary metabolites may serve as environmental cues that contribute to pathogen discrimination and avoidance.

Results

DAF-7/TGF-β is required for behavioral avoidance of *Pseudomonas aeruginosa*

We previously observed that mutants defective in the DAF-7/TGF-β pathway display enhanced susceptibility to infection by *P. aeruginosa* (Reddy et al., 2009). In the standard pathogenesis assay, *daf-7* mutants die faster than the wild-type strain N2 and exhibit a failure to avoid the bacterial lawn (Figures 1A and 1C). Initially, animals begin inside the lawn, but by 15 h wild-type N2 animals avoid the lawn of pathogenic bacteria, while *daf-7* mutants remain inside the lawn of *P. aeruginosa* (Figures 1C and 1D). In a modified pathogenesis assay in which *C. elegans* are unable to avoid the lawn of pathogenic bacteria, *daf-7* mutants display the same susceptibility phenotype as wild-type animals, demonstrating that the failure to avoid *P. aeruginosa* is the principal determinant in the susceptibility to infection of *daf-7* animals (Figure 1B). We also confirmed that *daf-7* animals were indeed being exposed to a higher dose of pathogenic bacteria by repeating the experiment with a *P. aeruginosa* lawn containing red fluorescent beads that serve as markers of the bacterial load in the intestine (Figure S1A).

Once secreted, DAF-7 binds to the TGF-β type I receptor DAF-1 and the TGF-β type II receptor DAF-4, which then act to antagonize the co-SMAD DAF-3 (Figure 1E) (Estevez et al., 1993; Georgi et al., 1990; Patterson et al., 1997). Other mutants in the DAF-7/TGF-β-signaling pathway such as *daf-1* and the R-SMAD *daf-8* also display *P. aeruginosa* avoidance defects (Figure S1B), and we observed complete suppression of the *daf-7(ok3125)* avoidance defect by a mutation in *daf-3* (Figure 1D). These results indicate that the DAF-7 pathway is specifically required for avoidance of *P. aeruginosa*, functioning through the canonical DAF-3 signaling pathway to promote survival by limiting host exposure to pathogenic bacteria.

P. aeruginosa induces *daf- 7* expression in the ASJ neuron pair and promotes avoidance behavior

The TGF-β ligand *daf-7* was previously shown to be expressed exclusively in the ASI pair of ciliated chemosensory neurons, with expression levels responsive to changes in the availability of standard *E. coli* food and *C. elegans* pheromones (Ren et al., 1996; Schackwitz et al., 1996). To monitor *daf-7* expression in the presence of *P. aeruginosa* we used a transgenic strain carrying a *daf-7p::gfp* transcriptional reporter. Unexpectedly, we observed that exposure to *P. aeruginosa* induced fluorescence in four cells—the ASI neuron pair as well as a second bilaterally symmetric pair of ciliated chemosensory neurons (Figures 2A–2B). Through co-localization experiments with the lipophilic dye DiI, we identified the additional cells as the ASJ chemosensory neurons (Figures 2C–2F). We quantified the *daf-7p::gfp* fluorescence increase in the ASJ neurons and found that the reporter was induced at least 1000-fold on *P. aeruginosa* relative to *E. coli* (Figure 2G). We also observed that the *daf-7p::gfp* fluorescence in the ASI neurons increased 2-fold on *P. aeruginosa* (Figure 2G).

We used fluorescent *in situ* hybridization of mRNA molecules to corroborate our observations made with the *daf-7p::gfp* transcriptional reporter. We did not detect

fluorescence in the ASJ neuron pair when the laboratory wild-type strain N2 was propagated on *E. coli* OP50 (Figures 2H and 2J). In contrast, upon exposure of *C. elegans* to *P. aeruginosa*, we observed *daf-7* mRNA expression in two additional cells corresponding to the ASJ neuron pair (Figures 2I and 2J). Confirming the specificity of the fluorescence for *daf-7* mRNA, we did not detect *daf-7* mRNA in a *daf-7(ok3125)* mutant strain carrying a 664 bp deletion, using probes designed to hybridize exclusively to the sequence within the deletion (Figure S2A). Of note, we observed that when the wild-type strain was propagated on *E. coli*, in addition to previously described expression in the ASI neuron pair, *daf-7* mRNA was also present in six other sensory neurons, which we identified using reporter co-localization experiments as the ADE neuron pair and the OLQ neurons (Figures 2H–2I and S2B–S2G). ADE and OLQ are mechanosensory neurons that have been implicated in bacterial food sensing (Hart et al., 1995; Sawin et al., 2000), and likely represent additional previously unknown sites of DAF-7/TGF- β expression.

To follow the kinetics of the endogenous *daf-7* transcriptional response to *P. aeruginosa* in the ASJ neurons, we fixed animals following exposures to *P. aeruginosa* ranging in duration from 3 min to 24 h and probed for *daf-7* mRNA. On *E. coli* or following a 3 min exposure to *P. aeruginosa* we did not detect *daf-7* mRNA in the ASJ neurons (Figure 2J). However after a 6 min exposure to *P. aeruginosa daf-7* mRNA was present in the ASJ neurons and did not appear to increase further over time (Figure 2J). The rapid kinetics of this transcriptional response, far faster than the kinetics of intestinal infection or aversive learning behavior (Tan et al., 1999; Zhang et al., 2005), led us to hypothesize that the ASJ chemosensory neurons may be responding directly to specific *P. aeruginosa* cues.

We determined that transgenic overexpression of *daf-7* under the native *daf-7* promoter or the ASJ-specific *trx-1* promoter, as well as under the ASI-specific *str-3* promoter, were each sufficient to restore wild-type pathogen avoidance and susceptibility in the *daf-7(ok3125)* mutant background (Figures 3A and 3C), consistent with the activity of DAF-7 as a secreted ligand. We also observed that the genetic ablation of the ASJ neuron pair conferred a partial deficit in *P. aeruginosa* avoidance and susceptibility (Figures 3B and 3D), demonstrating that the ASJ neurons are necessary for the complete protective response to *P. aeruginosa*. To determine if the ASJ-ablation avoidance phenotype was due to a loss of DAF-7 secretion from those neurons, we introduced mutations in the downstream co-SMAD *daf-3* that is epistatic to *daf-7* (Figure 1E). Mutant *daf-3* alleles were able to partially suppress the avoidance defect of both ASJ-ablation lines, consistent with the ASJ-ablation phenotype being due in part to a loss of *P. aeruginosa*-induced DAF-7 secretion (Figure 3D). These data establish a functional role for the induction of *daf-7* in the ASJ neuron pair upon exposure to *P. aeruginosa*.

DAF-7 signals to the RIM/RIC interneurons adjacent to the ASJ neurons to promote pathogen avoidance

To understand how expression of *daf-7* from the ASJ neurons promotes pathogen avoidance, we proceeded to examine the involvement of downstream signaling components of the canonical DAF-7/TGF-β pathway in the behavioral avoidance of *P. aeruginosa*. The *daf-1* gene encodes the TGF-β Type I receptor that binds DAF-7 and is expressed in over 80

neurons including ciliated sensory neurons, pharyngeal neurons, and interneurons (Gunther et al., 2000). We found that *daf-1* mutants, like *daf-7* mutants, are deficient in avoidance of *P. aeruginosa* (Figure 3E). Using *daf-1* mutant strains in which transgenic expression of *daf-1* is directed in subsets of neurons, we observed that *daf-1* expression under its native promoter or the panneuronal *egl-3* promoter rescued *P. aeruginosa* avoidance to wild-type levels, but no rescue was observed when *daf-1* was expressed in ~60 ciliated sensory neurons (including ASI and ASJ) using either the *osm-6* or *bbs-1* promoters (Figure 3E). Expression of *daf-1* in only the RIM/RIC interneurons under the *tdc-1* promoter was sufficient to restore pathogen avoidance behavior in the *daf-1* mutant to wild-type levels (Figure 3E). Previous work showed that DAF-1 also acts in the RIM/RIC interneurons to mediate wild-type development, feeding rate, and quiescence (Gallagher et al., 2013; Greer et al., 2008), suggesting that despite the broad expression of *daf-1* the RIM/RIC neurons may be the primary site of DAF-1 activity with regard to regulation of *C. elegans* behavior and physiology. The close proximity of the left and right ASJ neurons to the corresponding RIM/RIC interneurons on the ventral side of the amphid are in striking contrast to the location of the ASI neuron pair on the far dorsal side (White et al., 1986), and suggest an anatomical basis for how *P. aeruginosa* promotes enhanced DAF-7/TGF-β-dependent signaling (Figure 7D).

DAF-7 promotes pathogen avoidance through the modulation of aerotaxis behavior

DAF-7-dependent regulation of dauer entry, feeding rate, and fat storage similarly rely on repression of the co-SMAD DAF-3 in the RIM/RIC interneurons, but downstream regulation of each of these physiological processes diverges genetically and utilizes distinct sets of neurons (Greer et al., 2008). Mutations in the steroid hormone receptor *daf-12*, for example, are able to suppress the constitutive dauer entry phenotype of *daf-7* but not the increased fat storage or decreased feeding rate phenotypes. Similarly, mutations in the tyramine and octopamine synthesizing enzymes *tdc-1* and *tbh-1* suppress only the feeding rate phenotype of *daf-7*, while mutations in the $G_o\alpha$ signaling molecules *goa-1* and *dgk-1* suppress only the fat storage phenotype of *daf-7* (Greer et al., 2008). We determined that mutations in *daf-12, tdc-1, tbh-1, goa-1*, and *dgk-1* were all unable to suppress the avoidance phenotypes of *daf-7* mutants, indicating the existence of an additional signaling output by the RIM/RIC interneurons (Figure 3F).

In the presence of bacterial food, the laboratory wild-type strain of *C. elegans* N2 does not exhibit a distinct oxygen preference, and in particular does not avoid high atmospheric oxygen concentrations (i.e. 20% O_2). In contrast, *daf-7* mutants have altered aerotaxis behavior preferring oxygen concentrations near 8% and avoiding higher atmospheric oxygen levels (Chang et al., 2006). We have previously shown that the *P. aeruginosa* lawn is hypoxic, and that altered oxygen preference can affect bacterial lawn avoidance (Reddy et al., 2009; 2011). To determine whether a similar mechanism underlies the pathogen avoidance behavior promoted by *daf-7*, we introduced a mutation in the soluble guanylate cyclase *gcy-35*, which is responsible for responding to increases in oxygen concentration (Zimmer et al., 2009), and observed full suppression of the *daf-7* avoidance defect on *P. aeruginosa* (Figure 3F). In addition, we performed the pathogen avoidance assay in an oxygen chamber at low oxygen concentrations, such that the surrounding environment

would fall within the preferred oxygen concentration range of the animals. In this context *daf-7* mutants show no avoidance defect relative to wild-type animals, supporting our conclusion that *daf-7* mutants fail to avoid *P. aeruginosa* due to aberrant aerotaxis behavior (Figure S3A). We also conducted further experiments to demonstrate that the observed effects of DAF-7 on aerotaxis behavior and pathogen avoidance are not limited to the laboratory-adapted N2 strain (Figure S3B). Our model suggests that by activating *daf-7* expression in the ASJ neurons in response to *P. aeruginosa*, inhibition of DAF-3 activity in the adjacent RIM/RIC interneurons is increased, modifying the response of *C. elegans* to oxygen levels and promoting exit from the lawn of *P. aeruginosa*.

G protein-dependent signaling activates *daf-7* expression in the ASJ neuron pair in response to *P. aeruginosa*

The rapid kinetics and functional consequence of *P. aeruginosa*-induced *daf-7* expression in the ASJ neuron pair motivated use of the *daf-7p::gfp* reporter to identify signaling mechanisms coupling *P. aeruginosa* exposure to this robust transcriptional response. We began by analyzing mutants known to have reduced *daf-7* expression levels in the ASI neuron pair, such as the guanylate cyclase DAF-11 and the cyclic nucleotide-gated channel encoded by *tax-2/tax-4* (Chang et al., 2006; Murakami et al., 2001), which are downstream of G protein signaling in *C. elegans* chemosensory neurons (Bargmann, 2006). No *daf-7* expression was observed in either the ASI or ASJ neurons on *P. aeruginosa* in these mutant backgrounds, consistent with *daf-11*, *tax-2*, and *tax-4* acting upstream of *daf-7* expression in all tissues (Figures 4A–4D and S4A–S4C). These results suggest that the ASJ response to *P. aeruginosa* is downstream of G protein signaling and further motivate the identification of genes that specifically regulate *daf-7* expression in the ASJ neurons.

We performed a forward genetic screen to identify mutants in which the *daf-7p::gfp* reporter failed to be expressed in the ASJ neurons on *P. aeruginosa* but GFP fluorescence remained unchanged in the ASI neurons. One such mutant, *qd262* (Figures S4D–S4E), mapped to a region of chromosome V containing the G protein alpha subunit *gpa-3*. Sequencing revealed that the *qd262* mutant carries a missense mutation in *gpa-3* that converts a glycine residue (conserved from yeast to humans) into aspartic acid. Confirming the identity of the *qd262* mutant as an allele of *gpa-3*, we crossed the *gpa-3* deletion allele *pk35* into the *daf-7p::gfp* reporter and observed reduced fluorescence in the ASJ neurons on *P. aeruginosa* (Figures 4E and 4M). Mutants carrying a deletion in a second highly homologous G protein alpha subunit, *gpa-2*, also displayed reduced *daf-7p::gfp* fluorescence in ASJ (Figures 4F and 4M), and the *gpa-2 gpa-3* double mutant was completely deficient in the ASJ-response to *P. aeruginosa* (Figures 4G and 4M). Interestingly, the *gpa-2(pk16) gpa-3(pk35)* double mutant was still able to upregulate expression of *daf-7p::gfp* in the ASI neuron on *P. aeruginosa*, indicating that the ASJ and ASI responses to *P. aeruginosa* are genetically distinct (Figure 4N). The *C. elegans* nervous system is equipped with approximately 1,300 G protein-coupled receptors that act as chemoreceptors (Thomas and Robertson, 2008), and we hypothesize that GPA-3 and GPA-2 may be acting downstream of one or more GPCRs responsible for sensing *P. aeruginosa*.

gpa-3 is expressed in at least ten pairs of amphid sensory neurons (including ASJ), and its known functions include mediating responses to *C. elegans* pheromone in ASK, odorant attraction in AWA and AWC, and odorant avoidance in ASH (Hilliard et al., 2004; Jansen et al., 1999; Kim et al., 2009; Lans et al., 2004; Zwaal et al., 1997). To determine if GPA-3 acts cell-autonomously in the ASJ neurons to mediate the response to *P. aeruginosa*, we expressed wild-type copies of *gpa-3* cDNA under heterologous promoters in the *gpa-2(pk16) gpa-3(pk35)* background. Under control of either the pan-ciliated neuronal promoter *bbs-1*, or the ASJ-specific promoter *trx-1*, *gpa-3* cDNA was able to rescue the *daf-7* ASJ expression defect, indicating that GPA-3 acts cell-autonomously in ASJ to mediate the response to *P. aeruginosa* (Figures 4H–4I and S4F–S4I).

gpa-2 is reported to be expressed in only one pair of chemosensory neurons (AWC) and functions in the processes of olfaction and dauer induction (Lans et al., 2004; Zwaal et al., 1997). To determine the site of action for *gpa-2* in the response to *P. aeruginosa*, we expressed wild-type copies of *gpa-2* cDNA under heterologous promoters in the *gpa-2(pk16) gpa-3(pk35)* background. To our surprise, expression of *gpa-2* driven by either the pan-ciliated neuronal promoter *bbs-1* or the ASJ-specific promoter *trx-1* was able to rescue the *daf-7p*::*gfp* phenotype, but expression of *gpa-2* in the AWC neurons under the *ceh-36* promoter was not able to rescue the *gpa-2 gpa-3* mutant phenotype (Figures 4J–4L and S4J–S4K). This indicates that GPA-2, like GPA-3, also acts cell-autonomously in ASJ to induce *daf-7* expression in response to *P. aeruginosa*. To confirm that *gpa-2* was indeed expressed in the ASJ neurons we used single molecule FISH to probe for *gpa-2* mRNA. Using probes specific for *gpa-2*, we observed 5–10 mRNA molecules in each ASJ neuron (data not shown). This novel expression supports our neuron-specific rescue data and indicates that GPA-2 and GPA-3 act together in the ASJ neurons to activate *daf-7* expression in response to *P. aeruginosa*. Finally, we tested the *gpa-2 gpa-3* double mutant for a *P. aeruginosa* avoidance defect, and observed a partial deficit in lawn avoidance that we hypothesize is due to a loss of DAF-7 secretion from the ASJ neurons (Figure 4O). These experiments identify a conserved G protein signaling pathway that acts cell-autonomously in the ASJ neurons to induce *daf-7* expression in response to *P. aeruginosa*.

Chemosensory recognition of the *P. aeruginosa* secondary metabolites phenazine-1-carboxamide and pyochelin by the ASJ neuron pair of *C. elegans*

We next sought to identify the specific bacterial cues inducing expression of *daf-7* in the ASJ neuron pair of *C. elegans*. We observed that exposure of *C. elegans* to filtered *P. aeruginosa* supernatant was sufficient to induce *daf-7* expression (Figures 5A and 6A–6B). Furthermore, by testing supernatants from liquid cultures at various growth stages we determined that *P. aeruginosa* in stationary phase induced *daf-7* expression in ASJ neurons most dramatically (Figure 5A), leading us to hypothesize that specific secondary metabolites produced under high cell density were being sensed by *C. elegans*. Metabolite identification was accomplished via activity-guided fractionation followed by 2D NMR spectroscopic profiling. Supernatant from large volumes of stationary phase *P. aeruginosa* was fractionated using an automated chromatography system, and individual fractions were tested for activity in the *daf-7p*::*gfp* assay. 1D and 2D NMR (dqfCOSY, HSQC, HMBC) spectroscopic data of the active fractions were then analyzed. Such NMR spectroscopic

analysis of metabolome fractions of lowered complexity shifts focus onto testing individual identified components in bioassays, thereby reducing the need for further time-intensive purification (Taggi et al., 2004).

2D NMR spectra of the active fractions revealed the presence of pantolactone (Nakata et al., 2013), isovaleric acid (Niu et al., 2008), phenazine-1-carboxylic acid (Mehnaz et al., 2013), phenazine-1-carboxamide (PCN, see Table S1), the siderophore pyochelin (see Table S2) and phenyl acetic acid (Korsager et al., 2013) as major components (Figures 5B, S5A, and S5B), in addition to small quantities of monoacyl glycerides and β-hydroxy fatty acids. When synthetic and HPLC-purified samples of these compounds were tested, PCN and pyochelin displayed concentration-dependent activity in the *daf-7p*::*gfp* assay, regardless of solvent (Figures 6A and S6), whereas the other identified metabolites were not active in this assay. Furthermore, we found that other *P. aeruginosa*-produced phenazines (e.g. pyocyanin and phenazine-1-carboxylic acid) and pyoverdine, another unrelated *P. aeruginosa* siderophore, do not induce *daf-7* expression in the ASJ neurons (Figure 6A), indicating that general properties of these compounds are likely not the cause of their activity. We quantified the *daf-7p*::*gfp* fluorescence increase in the ASJ neurons following addition of pyochelin and PCN and found the response was similar to that induced by *P. aeruginosa* supernatant (Figure 6B). Interestingly we found that these compounds had no effect on *daf-7p*::*gfp* fluorescence in the ASI neurons, further decoupling the responses of the ASJ and ASI neurons to *P. aeruginosa* (Figure 6B).

Given the rapid transcriptional response of the ASJ neurons to the presence of *P. aeruginosa* secondary metabolites, we tested the ability of phenazine-1-carboxamide (PCN) to activate the ASJ neurons. We constructed a transgenic strain in which the genetically encoded calcium indicator GCaMP5 (Akerboom et al., 2012) is expressed exclusively in the ASJ neuron pair. Upon administration of PCN, but not the carrier control DMSO, we observed increased GCaMP5 fluorescence in both the ASJ cell body and ASJ ciliated projection that is exposed to the environment (Figures 6C–6D). We quantified the change in fluorescence in the ASJ cell body and observed a significant difference between PCN and the carrier control (Figures 6E–6F). These data suggest that ASJ may be sensing the *P. aeruginosa* metabolite PCN directly and, in turn, activating *daf-7* transcription.

Microbial discrimination and specificity in the chemosensory response to *P. aeruginosa*

In the natural environment *C. elegans* are unlikely to be presented with homogeneous bacterial lawns consisting of a single bacterial species, and so we wondered how sensitive the *daf-7p*::*gfp* response is to the concentration of *P. aeruginosa*. We created heterogeneous bacterial lawns consisting of *E. coli* and *P. aeruginosa* and assayed *daf-7p*::*gfp* fluorescence. We observed that the induction of *daf-7* expression does not function as a binary switch but rather can respond in a more subtle manner that is proportional to the fraction of *P. aeruginosa* present in the mixed *E. coli/P. aeruginosa* lawn (Figures 7A–7B). Interestingly, the *P. aeruginosa* concentration range over which *daf-7* is activated corresponds to the range sufficient to induce the *C. elegans* behavioral avoidance response (Figures 7A–7B).

Finally, we investigated how specific the induction of *daf-7* transcription in the ASJ neuron pair was to *P. aeruginosa* as compared to other environmental microbes. We exposed *daf-7p::gfp* animals to a wide array of bacterial species and strains, covering pathogenic and non-pathogenic alpha-, beta-, and gammaproteobacteria as well as gram-positive bacterial species. We observed that a number of non-*E. coli* species can induce *daf-7* expression in the ASJ neuron pair on the order of 10-fold, but that the response is 1–2 orders of magnitude greater upon exposure to *P. aeruginosa* PA14 (Figure 7C). This result indicates that the identity of the microbial species is the principal determinant in inducing *daf-7* expression in the ASJ neuron pair, likely due to the relatively species-specific production of *P. aeruginosa* metabolites PCN and pyochelin (see Discussion). The presence of low-level activity in bacterial strains other than *P. aeruginosa* is consistent with the existence of additional, unidentified bacterial determinants that also contribute to the induction of *daf-7* in the ASJ neuron pair.

PCN and pyochelin are secondary metabolites produced by *P. aeruginosa* at high cell density that promote biofilm formation in soil as well as chronic infections in human lungs (Cornelis and Dingemans, 2013; Price-Whelan et al., 2006). In *P. aeruginosa* production of phenazines and pyochelin are both positively regulated by GacA, a global activator of cell-density-dependent gene expression and virulence (Reimmann et al., 1997; Wei et al., 2013). We observed that the *P. aeruginosa gacA* mutant was deficient in inducing *daf-7p::gfp* expression in the ASJ neurons relative to wild-type bacteria (Figure 7C). As such, these molecules may serve as bacterial growth-stage-specific cues for *C. elegans*, alerting the host to the presence of bacteria in a “pathogenic state,” and inducing a correspondingly beneficial behavioral avoidance response.

Discussion

Our data suggest that *C. elegans* responds to secondary metabolites produced by bacterial pathogens using G protein signaling pathways in their chemosensory neurons. *C. elegans* lack the antigen-specific responses of vertebrate immunity, but the utilization of chemosensory neurons and the repertoire of an estimated 1,300 GPCRs may provide a means by which a simple host organism can detect microbial pathogens. Bacterial secondary metabolism can generate a wide range of molecules that are often largely specific with regard to producer organism and regulated by environmental and growth conditions. Redox-active phenazine-1-carboxamide and the siderophore pyochelin are two such secondary metabolites of *P. aeruginosa*, produced under conditions of high cell density and low oxygen. Interestingly, while a number of other bacterial species produce phenazines, such as *Burkholderia*, *Brevibacterium*, and *Streptomyces*, the modifying enzyme responsible for producing phenazine-1-carboxamide, *phzH*, is not part of the canonical phenazine operon, but rather found elsewhere in the genome and limited to *P. aeruginosa* and *P. chlororaphis* (Chin-A-Woeng et al., 2001; Mavrodi et al., 2001). Similarly, pyochelin production is restricted to *Pseudomonas* and *Burkholderia* species (Gross and Loper, 2009). As such, these two metabolites may act as pathogen-specific cues for *C. elegans* navigation, providing a molecular readout not only of the presence of *P. aeruginosa* itself, but the presence of *P. aeruginosa* in a “pathogenic state” that is more strongly associated with virulence.

Our data demonstrate that DAF-7 neuroendocrine signaling is necessary for the behavioral avoidance response to *P. aeruginosa*. The decision to occupy or avoid a lawn of *P. aeruginosa* integrates multiple sensory inputs including chemosensation of bacterial compounds, chemosensation of oxygen, and mechanosensation (Chang et al., 2011; Ha et al., 2010; Pradel et al., 2007; Reddy et al., 2009). Once *C. elegans* have learned to avoid a particular food source, a process that requires the association of bacterial infection with specific odors and occurs many hours after exposure to pathogenic bacteria (Zhang et al., 2005), they are confronted with conflicting environmental stimuli: the odor of pathogenic bacteria drives animals out of the lawn, while the relatively low oxygen concentration of the bacterial environment keeps animals inside the lawn. The DAF-7 pathway suppresses this latter tendency, and thus increasing the activity of DAF-7 in response to pathogenic bacteria promotes subsequent avoidance behavior. For *C. elegans*, which must balance attraction to bacterial food with avoidance of microbial pathogens, suppressing behaviors such as aerotaxis that keep the animal inside the bacterial lawn may be just as essential as activating behaviors that drive it away.

Whereas defining the connectivity of the *C. elegans* nervous system has provided the anatomical foundation for functional studies of neuronal circuitry (White et al., 1986), genetic studies of behavior have revealed pivotal roles for neuromodulators, such as neurotransmitters and neuropeptides, which modify the activity of synaptic circuits in response to environmental cues (Bargmann, 2012). Prior studies have illustrated how a change in the neuronal expression pattern of a single component of neuromodulator signaling can have dramatic effects on complex behavior (Lim et al., 2004; Pocock and Hobert, 2010). Our study establishes that patterns of neuromodulator expression and activity may be subject to dramatic modification by the microbial environment. There has been an emerging appreciation of the profound influence that the animal microbiota can have on host organisms (Clemente et al., 2012; Lyte, 2013), and our study provides a genetic, neuronal, chemical basis for how microbes may influence host neuroendocrine physiology and behavior.

Experimental Procedures

C. elegans Strains

C. elegans was maintained on *E. coli* OP50 as previously described (Brenner, 1974). Constitutive dauer strains were grown at the permissive temperature of 16°C until they had passed the dauer developmental decision. For assays in which a synchronized population of animals was required, strains were egg-prepped in bleach and arrested overnight in M9 buffer at the L1 larval stage. For a complete list of strains used in this study see Table S3.

daf-7p::gfp Induction Assays and Bacterial Strains

For testing the dynamics of *daf-7* expression on *P. aeruginosa* PA14, an overnight culture of PA14 was grown in 2–3 mL LB at 37°C, and the following morning 7 μL of culture was seeded onto 3.5 cm SKA plates as previously described (Tan et al., 1999). PA14 plates were grown overnight at 37°C and then grown for an additional day at room temperature. Animals at the L4 larval stage were then picked onto the center of the bacterial lawn, incubated at

25°C, and scored for changes in GFP expression 15–20 h later. Cell identification was performed using the lipophilic dye DiI from Molecular Probes. Images were acquired with an Axioimager Z1 microscope using animals anaesthetized in 50 mM sodium azide. To quantify GFP fluorescence animals were imaged at 40× magnification and the maximum intensity value within the ASJ neuron was determined using FIJI software. The same procedure (with the indicated modifications) was followed for: *Escherichia coli* OP50, *Serratia marcescens* DB10, *Bacillus subtilis* PY79, *Comamonas sp*. DA1877, *Enterococcus faecalis* OG1RF (grown overnight in Brain Heart Infusion Broth), and *Staphylococcus aureus* NCTC8325 (grown overnight in Tryptic Soy Broth). To test the activity of bacterial supernatant, fractionated supernatant, and purified compounds, 3.5 cm SKA plates were seeded with 5 μL *E. coli* OP50. Prior to adding *C. elegans*, 25 μL of test material was added to the bacterial lawn and allowed to dry. All compounds were dissolved in DMSO. To generate bacterial lawns that contained mixtures of *E. coli* and *P. aeruginosa*, plates were seeded with *E. coli* and allowed to grow for two days as above, at which time 7 μL of liquid *P. aeruginosa* culture (diluted to varying degrees) was added to the *E. coli* lawn and allowed to dry. After the experiment had concluded the fraction of the lawn corresponding to each bacterial species was measured by counting CFUs of *E. coli* and *P. aeruginosa* (distinguished by colony morphology).

P. aeruginosa Avoidance and Killing Assays

Plates for *P. aeruginosa* avoidance assays were prepared as above. 30 animals at the L4 larval stage were transferred to the center of PA14 lawns, incubated at 25°C, and scored for avoidance 15 h later. For avoidance experiments in hypoxia, plates were placed in a Coy Laboratory Products Inc. Hypoxic In Vitro Cabinet and incubated at 1%–4% O_2 at room temperature. Plates for measuring accumulation of red fluorescent beads were prepared as above with addition of Fluoresbrites 0.2 μm microspheres (Polyscience, Inc.) to the PA14 culture prior to seeding at a ratio of 50:1 (bacteria:beads). Plates for *P. aeruginosa* slow killing assays were prepared as above with the addition of 50 μg/mL 5-fluorodeoxyuridine (FUdR). 30 animals at the L4 larval stage were transferred to the center of PA14 lawns, incubated at 25°C, and scored for killing over the course of 5 days. For “Big Lawn” slow killing assays the following modifications were made: 15 μL of PA14 culture was spread to the edges of the SKA plate and 75 animals were added to each plate. Statistical analysis was performed using GraphPad Prism Software.

Single Molecule Fluorescent *In Situ* Hybridization

smFISH was performed as previously described (Raj et al., 2008). Briefly, *C. elegans* were fixed in 4% formaldehyde for 45 min at room temperature. After washing with PBS, larvae were resuspended in 70% EtOH and incubated overnight at 4°C. The following day fixed larvae were transferred into hybridization solution with the smFISH probe and incubated overnight at 30°C. The *daf-7* and *gpa-2* probes were constructed by pooling 25 unique DNA oligos that tile the coding regions deleted in the *daf-7(ok3125)* and *gpa-2(pk16)* mutants and coupling them to Cy5 dye. For a complete list of oligos see Table S4. Images were acquired with a Nikon Eclipse Ti Inverted Microscope outfitted with a Princeton Instruments PIXIS 1024 camera. Data were analyzed using FIJI software; images presented in Figures 2H, 2I, and S2A are maximum intensity z-projections of 30 stacked exposures.

Generation of Transgenic Animals

The *daf-7* promoter (3.1 kb), *trx-1* promoter (1.1 kb) (Fierro González et al., 2011), *str-3* promoter (2.8 kb), and *ceh-36* promoter (<1 kb) (Kim et al., 2010) were amplified by PCR from genomic DNA. The *bbs-1* promoter (1.9 kb) was amplified by PCR from plasmid pKA40 (laboratory of K. Ashrafi). *daf-7* cDNA was amplified by PCR from an ORFeome RNAi clone. *gpa-3* and *gpa-2* cDNAs were amplified by PCR from cDNA generated with an Ambion RETROscript Kit. The GCaMP5G gene was amplified from Plasmid 31788: pCMV-GCaMP5G (Addgene). The *unc-54* 3-prime UTR was amplified by PCR from Fire Vector pPD95.75. DNA constructs (promoter::cDNA::*unc-54* 3'UTR) were synthesized using PCR fusion as previously described (Hobert, 2002). PCR fusion products were cloned into pGEM-T Easy plasmids, sequenced to confirm identity, and injected into animals at a concentration of 50 ng/μL along with a plasmid carrying either *ges-1p::gfp* or *ofm-1p::gfp* (50 ng/μL). At least three independent transgenic lines were analyzed for each rescue construct. For a complete list of primers used in this study see Table S4.

Biochemical Identification of *P. aeruginosa* Metabolites

To generate *P. aeruginosa* supernatant, overnight bacterial cultures were grown in 500 mL LB at 37°C shaking at 200 rpm. Once the cultures had reached OD_{600} = 3.0 they were passed through a 0.22 μm PES filter system. The filtrate was lyophilized and the residue was extracted twice with 50 mL of 4:1 dichloromethane:methanol mixture over 12 h. The resulting suspension was centrifuged at 4,750 rpm at 4°C for 15 min and the supernatant liquid was collected. The solvent was evaporated *in vacuo* at room temperature to produce the *P. aeruginosa* supernatant extract used for chromatographic separations and analysis. For details, see Supplemental Experimental Procedures. NMR spectra were recorded on a Varian Inova 600 MHz NMR spectrometer equipped with an HCN indirect detection probe. Spectra were baseline corrected, phased and calibrated to the solvent peak ($CHCl_3$ singlet at 7.26 ppm) using Varian VNMR and MestreLab's Mnova software packages. Non-gradient phase-cycled double-quantum filtered correlation spectroscopy (DQF-COSY) spectra were acquired using the following parameters: 0.6 s acquisition time, 512 complex increments, 16 scans per increment. DQF-COSY spectra were zero filled to 8,192 × 4,096, and 90°-shifted sine bell window functions were applied in both dimensions before Fourier transformation. Heteronuclear single quantum coherence spectroscopy (HSQC) and heteronuclear multiple bond correlation spectroscopy (HMBC) spectra were acquired using the following parameters: 0.25 s acquisition time, 400–600 complex increments, 16 scans per increment. HSQC and HMBC spectra were zero filled to 2,048 × 2,048, and 90°-shifted sine bell window functions were applied in both dimensions. Unit mass-resolution HPLC-MS was performed using an Agilent 1100 Series HPLC system equipped with a diode array detector and connected to a Quattro II mass spectrometer (Micromass/Waters). MassLynx software was used for MS data acquisition and processing. UV-Vis spectra were recorded on Agilent Technologies 8453 UV-Vis spectrophotometer. For testing the activity of candidate compounds, phenazine-1-carboxamide was purchased from Princeton Biomolecular Research (PBMR030086), phenazine-1-carboxylic acid was purchased from Apollo Scientific (OR01490), pyochelin was purchased from Cfm Oskar Tropitzsch

(164104-31-8/164104-32-9), and pyocyanin (P0046) and pyoverdine (P8374) were purchased from Sigma-Aldrich.

Calcium Imaging

To measure the activity of the ASJ neurons GCaMP5G was expressed exclusively in the ASJ neurons under the *trx-1* promoter. Animals were immobilized on NGM agar pads using Surgi-lock 2oc instant tissue adhesive (Meridian) and imaged at 40X using a Zeiss AxioVert S100 inverted microscope outfitted with an Andor iXon EMCCD camera. Ten seconds after imaging had begun approximately 3 μL of stimulant (either PCN 10 mg/mL or DMSO) was added to the agar pad. In Figures 6C–6F time = 0 refers to the addition of stimulant. Data were analyzed using custom MATLAB software written by Nikhil Bhatla.

Supplementary Material

Refer to Web version on PubMed Central for supplementary material.

Acknowledgments

We thank J. Alcedo, K. Ashrafi, F. Ausubel, H. R. Horvitz, the *C. elegans* Knockout Consortium, and the *Caenorhabditis* Genetics Center (which is supported by the NIH, Office of the Director) for providing strains and reagents. We thank N. Bhatla, C. Engert, C. Pender, and S. Sando for technical assistance. J.D.M. was supported by a Graduate Research Fellowship from the National Science Foundation. This study was supported by the NIH (GM084477 to D.H.K. and GM088290 to F.C.S.) and an Ellison New Scholar Award (to D.H.K.).

References

Akerboom J, Chen TW, Wardill TJ, Tian L, Marvin JS, Mutlu S, Calderon NC, Esposti F, Borghuis BG, Sun XR, et al. Optimization of a GCaMP Calcium Indicator for Neural Activity Imaging. Journal of Neuroscience. 2012; 32:13819–13840. [PubMed: 23035093]

Avery L, Horvitz HR. Effects of starvation and neuroactive drugs on feeding in Caenorhabditis elegans. J. Exp. Zool. 1990; 253:263–270. [PubMed: 2181052]

Bargmann CI. Chemosensation in C. elegans. WormBook. 2006:1–29. [PubMed: 18050433]

Bargmann CI. Beyond the connectome: how neuromodulators shape neural circuits. Bioessays. 2012; 34:458–465. [PubMed: 22396302]

Beale E, Li G, Tan MW, Rumbaugh KP. Caenorhabditis elegans Senses Bacterial Autoinducers. Applied and Environmental Microbiology. 2006; 72:5135–5137. [PubMed: 16820523]

Brenner S. The genetics of Caenorhabditis elegans. Genetics. 1974; 77:71–94. [PubMed: 4366476]

Chang AJ, Chronis N, Karow DS, Marletta MA, Bargmann CI. A Distributed Chemosensory Circuit for Oxygen Preference in C. elegans. Plos Biol. 2006; 4:e274. [PubMed: 16903785]

Chang HC, Paek J, Kim DH. Natural polymorphisms in C. elegans HECW-1 E3 ligase affect pathogen avoidance behaviour. Nature. 2011; 480:525–529. [PubMed: 22089131]

Chin-A-Woeng TF, Thomas-Oates JE, Lugtenberg BJ, Bloemberg GV. Introduction of the phzH gene of Pseudomonas chlororaphis PCL1391 extends the range of biocontrol ability of phenazine-1-carboxylic acid-producing Pseudomonas spp. strains. Mol. Plant Microbe Interact. 2001; 14:1006–1015.

Clemente JC, Ursell LK, Parfrey LW, Knight R. The impact of the gut microbiota on human health: an integrative view. Cell. 2012; 148:1258–1270. [PubMed: 22424233]

Cornelis P, Dingemans J. Pseudomonas aeruginosa adapts its iron uptake strategies in function of the type of infections. Front Cell Infect Microbiol. 2013; 3:75. [PubMed: 24294593]

de Bono M, Tobin DM, Davis MW, Avery L, Bargmann CI. Social feeding in Caenorhabditis elegans is induced by neurons that detect aversive stimuli. Nature. 2002; 419:899–903. [PubMed: 12410303]

Estevez M, Attisano L, Wrana JL, Albert PS, Massagué J, Riddle DL. The daf-4 gene encodes a bone morphogenetic protein receptor controlling C. elegans dauer larva development. Nature. 1993; 365:644–649. [PubMed: 8413626]

Félix M-A, Duveau F. Population dynamics and habitat sharing ofnatural populations of Caenorhabditis elegans andC. briggsae. BMC Biol. 2012; 10:59. [PubMed: 22731941]

Fierro González JC, Cornils A, Alcedo J, Miranda-Vizuete A, Swoboda P. The Thioredoxin TRX-1 Modulates the Function of the Insulin-Like Neuropeptide DAF-28 during Dauer Formation in Caenorhabditis elegans. PLoS ONE. 2011; 6:e16561. [PubMed: 21304598]

Gallagher T, Kim J, Oldenbroek M, Kerr R, You Y-J. ASI Regulates Satiety Quiescence in C. elegans. Journal of Neuroscience. 2013; 33:9716–9724. [PubMed: 23739968]

Georgi LL, Albert PS, Riddle DL. daf-1, a C. elegans gene controlling dauer larva development, encodes a novel receptor protein kinase. Cell. 1990; 61:635–645. [PubMed: 2160853]

Greer ER, Pérez CL, Van Gilst MR, Lee BH, Ashrafi K. Neural and Molecular Dissection of a C. elegans Sensory Circuit that Regulates Fat and Feeding. Cell Metabolism. 2008; 8:118–131. [PubMed: 18680713]

Gross H, Loper JE. Genomics of secondary metabolite production by Pseudomonas spp. Nat Prod Rep. 2009; 26:1408–1446. [PubMed: 19844639]

Gunther CV, Georgi LL, Riddle DL. A Caenorhabditis elegans type I TGF beta receptor can function in the absence of type II kinase to promote larval development. Development. 2000; 127:3337–3347. [PubMed: 10887089]

Gusarov I, Gautier L, Smolentseva O, Shamovsky I, Eremina S, Mironov A, Nudler E. Bacterial nitric oxide extends the lifespan of C. elegans. Cell. 2013; 152:818–830. [PubMed: 23415229]

Ha H-I, Hendricks M, Shen Y, Gabel CV, Fang-Yen C, Qin Y, Colón-Ramos D, Shen K, Samuel ADT, Zhang Y. Functional Organization of a Neural Network for Aversive Olfactory Learning in Caenorhabditis elegans. Neuron. 2010; 68:1173–1186. [PubMed: 21172617]

Hart AC, Sims S, Kaplan JM. Synaptic code for sensory modalities revealed by C. elegans GLR-1 glutamate receptor. Nature. 1995; 378:82–85. [PubMed: 7477294]

Hedgecock EM, Russell RL. Normal and mutant thermotaxis in the nematode Caenorhabditis elegans. Proc. Natl. Acad. Sci. U.S.a. 1975; 72:4061–4065. [PubMed: 1060088]

Hilliard MA, Bergamasco C, Arbucci S, Plasterk RHA, Bazzicalupo P. Worms taste bitter: ASH neurons, QUI-1, GPA-3 and ODR-3 mediate quinine avoidance in Caenorhabditis elegans. Embo J. 2004; 23:1101–1111. [PubMed: 14988722]

Hobert O. PCR fusion-based approach to create reporter gene constructs for expression analysis in transgenic C. elegans. BioTechniques. 2002; 32:728–730. [PubMed: 11962590]

Jansen G, Thijssen KL, Werner P, van der Horst M, Hazendonk E, Plasterk RH. The complete family of genes encoding G proteins of Caenorhabditis elegans. Nat. Genet. 1999; 21:414–419. [PubMed: 10192394]

Kim K, Kim R, Sengupta P. The HMX/NKX homeodomain protein MLS-2 specifies the identity of the AWC sensory neuron type via regulation of the ceh-36 Otx gene in C. elegans. Development. 2010; 137:963–974. [PubMed: 20150279]

Kim K, Sato K, Shibuya M, Zeiger DM, Butcher RA, Ragains JR, Clardy J, Touhara K, Sengupta P. Two Chemoreceptors Mediate Developmental Effects of Dauer Pheromone in C. elegans. Science. 2009; 326:994–998. [PubMed: 19797623]

Korsager S, Taaning RH, Skrydstrup T. Effective palladium-catalyzed hydroxycarbonylation of aryl halides with substoichiometric carbon monoxide. J. Am. Chem. Soc. 2013; 135:2891–2894. [PubMed: 23398204]

Lans H, Rademakers S, Jansen G. A network of stimulatory and inhibitory Galpha-subunits regulates olfaction in Caenorhabditis elegans. Genetics. 2004; 167:1677–1687. [PubMed: 15342507]

Lim MM, Wang Z, Olazábal DE, Ren X, Terwilliger EF, Young LJ. Enhanced partner preference in a promiscuous species by manipulating the expression of a single gene. Nature. 2004; 429:754–757. [PubMed: 15201909]

Lyte M. Microbial Endocrinology in the Microbiome-Gut-Brain Axis: How Bacterial Production and Utilization of Neurochemicals Influence Behavior. PLoS Pathog. 2013; 9:e1003726. [PubMed: 24244158]

MacNeil LT, Watson E, Arda HE, Zhu LJ, Walhout AJM. Diet-induced developmental acceleration independent of TOR and insulin in C. elegans. Cell. 2013; 153:240–252. [PubMed: 23540701]

Mavrodi DV, Bonsall RF, Delaney SM, Soule MJ, Phillips G, Thomashow LS. Functional analysis of genes for biosynthesis of pyocyanin and phenazine-1-carboxamide from Pseudomonas aeruginosa PAO1. J. Bacteriol. 2001; 183:6454–6465. [PubMed: 11591691]

Mehnaz S, Saleem RSZ, Yameen B, Pianet I, Schnakenburg G, Pietraszkiewicz H, Valeriote F, Josten M, Sahl H-G, Franzblau SG, et al. Lahorenoic acids A–C, ortho-dialkyl-substituted aromatic acids from the biocontrol strain Pseudomonas aurantiaca PB-St2. J. Nat. Prod. 2013; 76:135–141. [PubMed: 23402329]

Milward K, Busch KE, Murphy RJ, de Bono M, Olofsson B. Neuronal and molecular substrates for optimal foraging in Caenorhabditis elegans. Proceedings of the National Academy of Sciences. 2011; 108:20672–20677.

Murakami M, Koga M, Ohshima Y. DAF-7/TGF-beta expression required for the normal larval development in C. elegans is controlled by a presumed guanylyl cyclase DAF-11. Mech. Dev. 2001; 109:27–35. [PubMed: 11677050]

Nakata K, Gotoh K, Ono K, Futami K, Shiina I. Kinetic resolution of racemic 2-hydroxy-γ-butyrolactones by asymmetric esterification using diphenylacetic acid with pivalic anhydride and a chiral acyl-transfer catalyst. Org. Lett. 2013; 15:1170–1173. [PubMed: 23461674]

Niu DF, Xiao LP, Zhang AJ, Zhang GR, Tan QY, Lu JX. Electrocatalytic carboxylation of aliphatic halides at silver cathode in acetonitrile. Tetrahedron. 2008

Patterson GI, Koweek A, Wong A, Liu Y, Ruvkun G. The DAF-3 Smad protein antagonizes TGF-beta-related receptor signaling in the Caenorhabditis elegans dauer pathway. Genes & Development. 1997; 11:2679–2690. [PubMed: 9334330]

Pocock R, Hobert O. Hypoxia activates a latent circuit for processing gustatory information in C. elegans. Nature Publishing Group. 2010; 13:610–614.

Pradel E, Zhang Y, Pujol N, Matsuyama T, Bargmann CI, Ewbank JJ. Detection and avoidance of a natural product from the pathogenic bacterium Serratia marcescens by Caenorhabditis elegans. Proc. Natl. Acad. Sci. U.S.a. 2007; 104:2295–2300. [PubMed: 17267603]

Price-Whelan A, Dietrich LEP, Newman DK. Rethinking “secondary” metabolism: physiological roles for phenazine antibiotics. Nat Chem Biol. 2006; 2:71–78. [PubMed: 16421586]

Pujol N, Link EM, Liu LX, Kurz CL, Alloing G, Tan MW, Ray KP, Solari R, Johnson CD, Ewbank JJ. A reverse genetic analysis of components of the Toll signaling pathway in Caenorhabditis elegans. Curr. Biol. 2001; 11:809–821. [PubMed: 11516642]

Raj A, van den Bogaard P, Rifkin SA, van Oudenaarden A, Tyagi S. Imaging individual mRNA molecules using multiple singly labeled probes. Nat Meth. 2008; 5:877–879.

Reddy KC, Andersen EC, Kruglyak L, Kim DH. A polymorphism in npr-1 is a behavioral determinant of pathogen susceptibility in C. elegans. Science. 2009; 323:382–384. [PubMed: 19150845]

Reddy KC, Hunter RC, Bhatla N, Newman DK, Kim DH. Caenorhabditis elegans NPR-1-mediated behaviors are suppressed in the presence of mucoid bacteria. Proceedings of the National Academy of Sciences. 2011; 108:12887–12892.

Reimmann C, Beyeler M, Latifi A, Winteler H, Foglino M, Lazdunski A, Haas D. The global activator GacA of Pseudomonas aeruginosa PAO positively controls the production of the autoinducer N-butyryl-homoserine lactone and the formation of the virulence factors pyocyanin, cyanide, and lipase. Mol Microbiol. 1997; 24:309–319. [PubMed: 9159518]

Ren P, Lim CS, Johnsen R, Albert PS, Pilgrim D, Riddle DL. Control of C. elegans larval development by neuronal expression of a TGF-beta homolog. Science. 1996; 274:1389–1391. [PubMed: 8910282]

Rivière S, Challet L, Fluegge D, Spehr M, Rodriguez I. Formyl peptide receptor-like proteins are a novel family of vomeronasal chemosensors. Nature. 2009; 459:574–577. [PubMed: 19387439]

Sawin ER, Ranganathan R, Horvitz HR. C. elegans locomotory rate is modulated by the environment through a dopaminergic pathway and by experience through a serotonergic pathway. Neuron. 2000; 26:619–631. [PubMed: 10896158]

Schackwitz WS, Inoue T, Thomas JH. Chemosensory neurons function in parallel to mediate a pheromone response in C. elegans. Neuron. 1996; 17:719–728. [PubMed: 8893028]

Shaw WM, Luo S, Landis J, Ashraf J, Murphy CT. The C. elegans TGF-β Dauer Pathway Regulates Longevity via Insulin Signaling. Current Biology. 2007; 17:1635–1645. [PubMed: 17900898]

Shtonda BB, Avery L. Dietary choice behavior in Caenorhabditis elegans. J. Exp. Biol. 2006; 209:89–102. [PubMed: 16354781]

Stensmyr MC, Dweck HKM, Farhan A, Ibba I, Strutz A, Mukunda L, Linz J, Grabe V, Steck K, Lavista-Llanos S, et al. A conserved dedicated olfactory circuit for detecting harmful microbes in Drosophila. Cell. 2012; 151:1345–1357. [PubMed: 23217715]

Swanson MM, Riddle DL. Critical periods in the development of the Caenorhabditis elegans dauer larva. Dev. Biol. 1981; 84:27–40. [PubMed: 7250500]

Taggi AE, Meinwald J, Schroeder FC. A new approach to natural products discovery exemplified by the identification of sulfated nucleosides in spider venom. J. Am. Chem. Soc. 2004; 126:10364–10369. [PubMed: 15315451]

Tan MW, Mahajan-Miklos S, Ausubel FM. Killing of Caenorhabditis elegans by Pseudomonas aeruginosa used to model mammalian bacterial pathogenesis. Proc. Natl. Acad. Sci. U.S.a. 1999; 96:715–720. [PubMed: 9892699]

Thomas JH, Robertson HM. The Caenorhabditis chemoreceptor gene families. BMC Biol. 2008; 6:42. [PubMed: 18837995]

Watson E, MacNeil LT, Ritter AD, Yilmaz LS, Rosebrock AP, Caudy AA, Walhout AJM. Interspecies Systems Biology Uncovers Metabolites Affecting C. elegans GeneExpression and Life History Traits. Cell. 2014; 156:759–770. [PubMed: 24529378]

Wei X, Huang X, Tang L, Wu D, Xu Y. Global Control of GacA in Secondary Metabolism, Primary Metabolism, Secretion Systems, and Motility in the Rhizobacterium Pseudomonas aeruginosa M18. J. Bacteriol. 2013; 195:3387–3400. [PubMed: 23708134]

White JG, Southgate E, Thomson JN, Brenner S. The structure of the nervous system of the nematode Caenorhabditis elegans. Philos. Trans. R. Soc. Lond., B, Biol. Sci. 1986; 314:1–340. [PubMed: 22462104]

Zhang X, Zhang Y. DBL-1, a TGF-β, is essential for Caenorhabditis elegans aversive olfactory learning. Proceedings of the National Academy of Sciences. 2012; 109:17081–17086.

Zhang Y, Lu H, Bargmann CI. Pathogenic bacteria induce aversive olfactory learning in Caenorhabditis elegans. Nature. 2005; 438:179–184. [PubMed: 16281027]

Zimmer M, Gray JM, Pokala N, Chang AJ, Karow DS, Marletta MA, Hudson ML, Morton DB, Chronis N, Bargmann CI. Neurons detect increases and decreases in oxygen levels using distinct guanylate cyclases. Neuron. 2009; 61:865–879. [PubMed: 19323996]

Zugasti O, Ewbank JJ. Neuroimmune regulation of antimicrobial peptide expression by a noncanonical TGF-β signaling pathway in Caenorhabditis elegans epidermis. Nat Immunol. 2009; 10:249–256. [PubMed: 19198592]

Zwaal RR, Mendel JE, Sternberg PW, Plasterk RH. Two neuronal G proteins are involved in chemosensation of the Caenorhabditis elegans Dauer-inducing pheromone. Genetics. 1997; 145:715–727. [PubMed: 9055081]

Highlights

- *C. elegans* chemosensory neurons respond to specific bacterial secondary metabolites
- Host neuromodulator gene expression pattern is altered by the microbial environment
- Detection of *P. aeruginosa* metabolites promotes protective behavioral avoidance

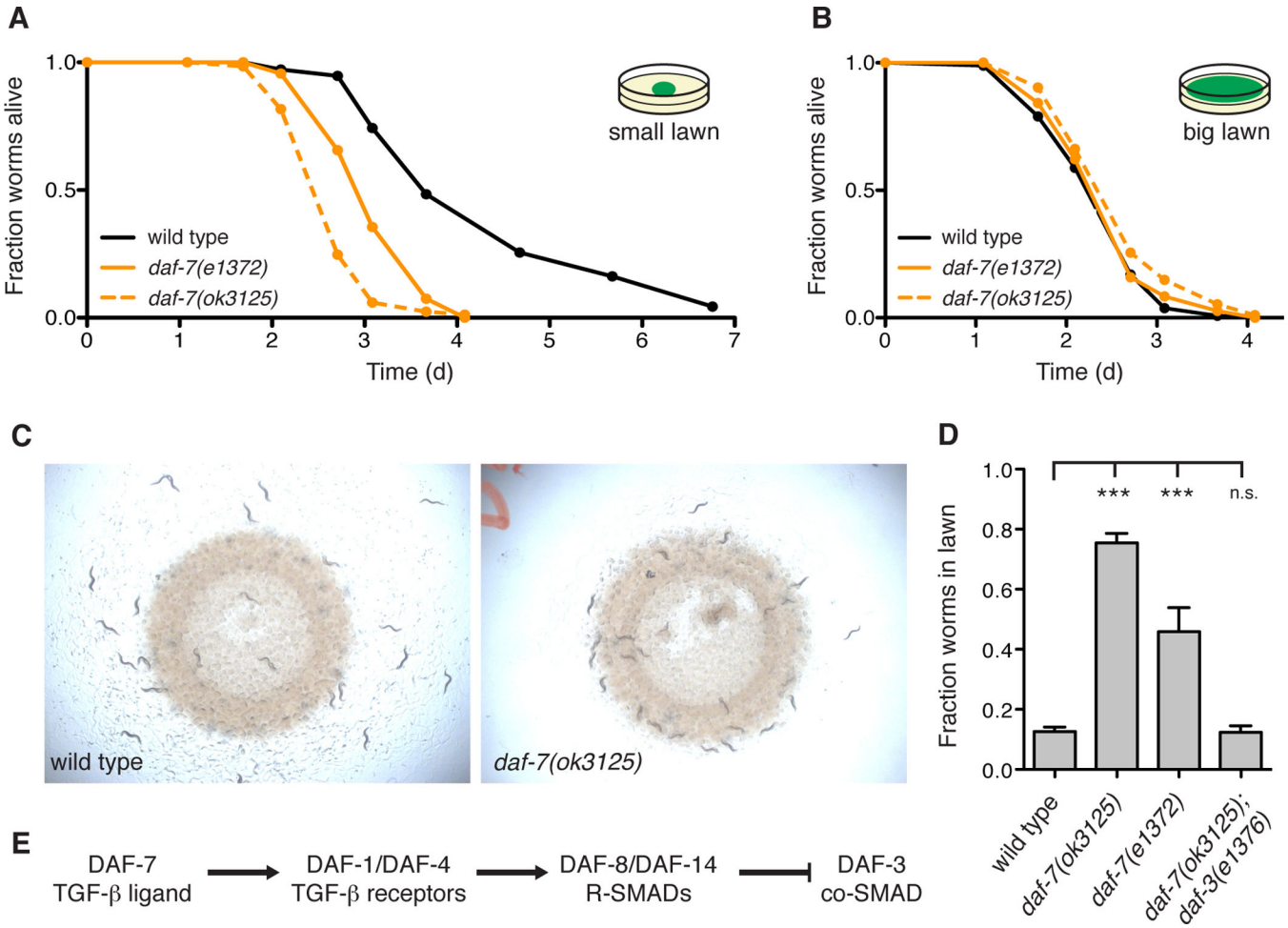

Figure 1. DAF-7/TGF-β is required for the protective behavioral avoidance response to *P. aeruginosa*

(A) Fraction animals alive after being transferred to plates seeded with *P. aeruginosa* strain PA14. (B) Fraction animals alive after being transferred to a "Big Lawn" of *P. aeruginosa* in which the bacteria has been spread to the edges of the plate. All data points represent the average of at least three independent replicates. (C) Photographs of wild-type and *daf-7* animals after 15 h exposure to *P. aeruginosa*. (D) Lawn occupancy of animals on *P. aeruginosa* after 15 h. (E) The canonical DAF-7/TGF-β signaling pathway in C. elegans. *** $P < 0.001$ as determined by one-way ANOVA followed by Dunnett's Multiple Comparison Test. n.s. = not significant. Values represent means of at least three independent experiments. Error bars indicate standard error. See also Figure S1.

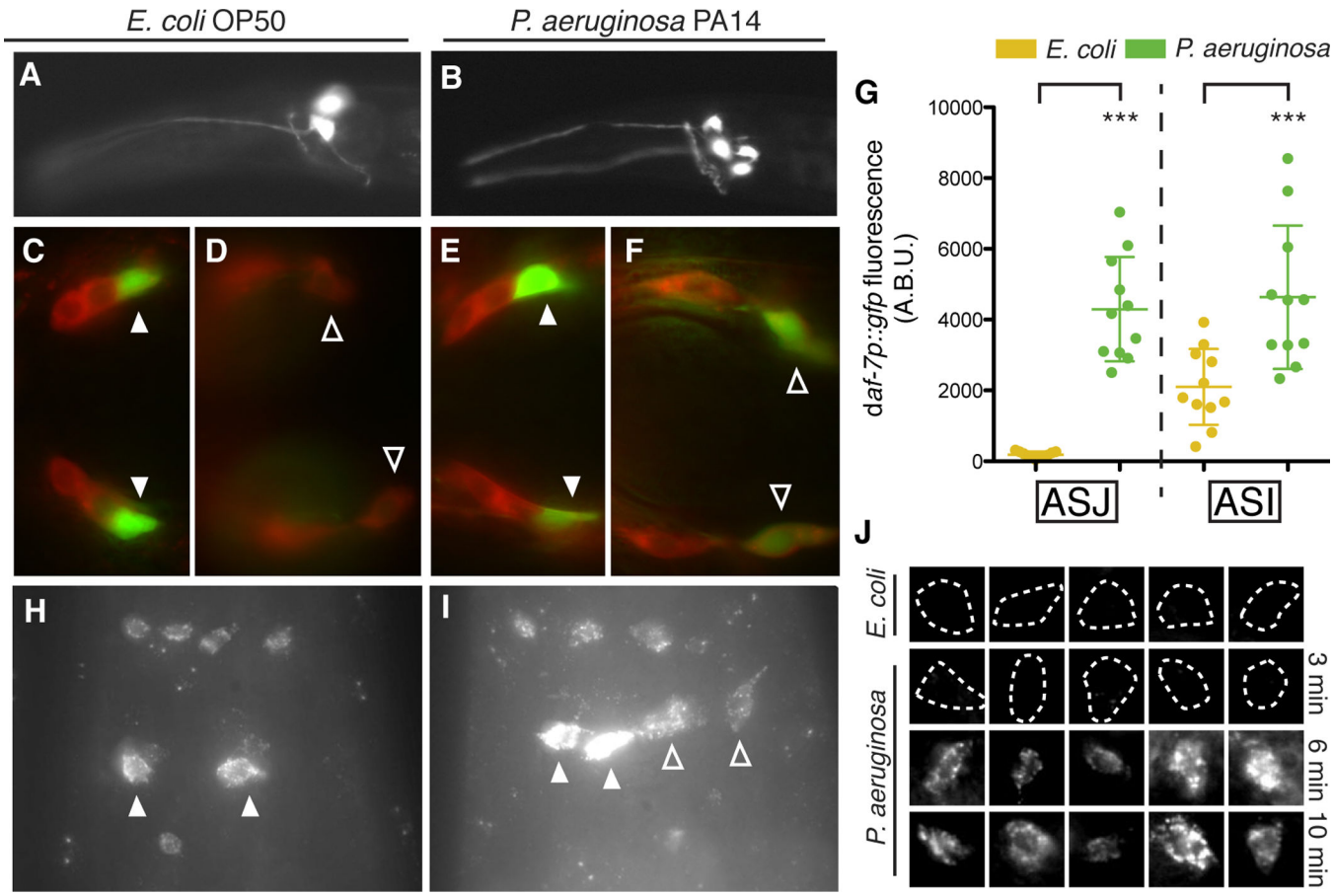

Figure 2. *daf-7* expression is induced in the ASJ neurons upon exposure to *P. aeruginosa*

(A–B) *daf-7p*::*gfp* expression pattern in *C. elegans on E. coli* (A) and *P. aeruginosa* (B). (C–F) Co-localization of *daf-7p*::*gfp* expression and DiI staining (red) in animals on *E. coli*, dorsal view (C) and ventral view (D), and in animals on *P. aeruginosa*, dorsal view (E) and ventral view (F). Filled triangles indicate ASI neurons; empty triangles indicate ASJ neurons. (G) Maximum fluorescence values of *daf-7p*::*gfp* in the ASJ or ASI neurons after 16 h exposure to indicated bacteria. *** $P < 0.001$ as determined by one-way ANOVA followed by Tukey's Multiple Comparison Test. Error bars indicate standard deviation. (H–I) *daf-7* FISH in wild-type N2 animals on *E. coli* (H) and *P. aeruginosa* (I). Filled triangles indicate ASI neurons; empty triangles indicate ASJ neurons. Additional cells expressing *daf-7* mRNA are the OLQ neurons (top) and the ADE neurons (bottom). (J) *daf-7* FISH in the ASJ neurons (co-localized with *trx-1p*::*gfp*) on *E. coli* and *P. aeruginosa* after various exposure times. Dashed lines indicate cell boundaries. Each image represents an individual animal. See also Figure S2.

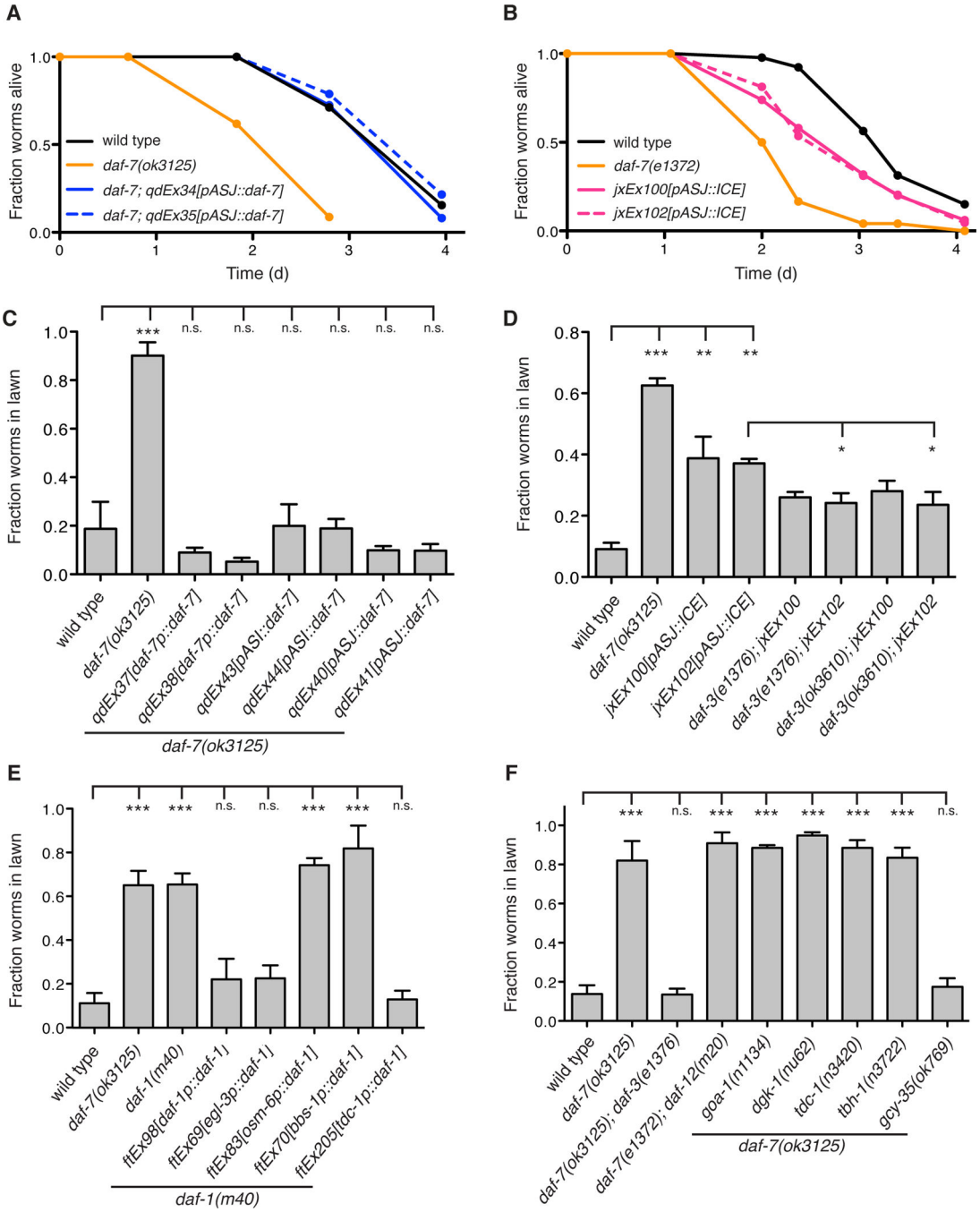

Figure 3. DAF-7 from the ASJ neuron pair signals to the RIM/RIC interneurons to alter aerotaxis behavior and promote avoidance of *P. aeruginosa*

(A–B) Fraction animals alive after being transferred to plates seeded with *P. aeruginosa*. All data points represent the average of at least three independent replicates. (C–F) Lawn occupancy of animals on *P. aeruginosa* after 15 h. *** $P < 0.001$, ** $P < 0.01$, * $P < 0.05$ as determined by one-way ANOVA followed by Dunnett's Multiple Comparison Test. n.s. = not significant. Error bars indicate standard deviation. See also Figure S3.

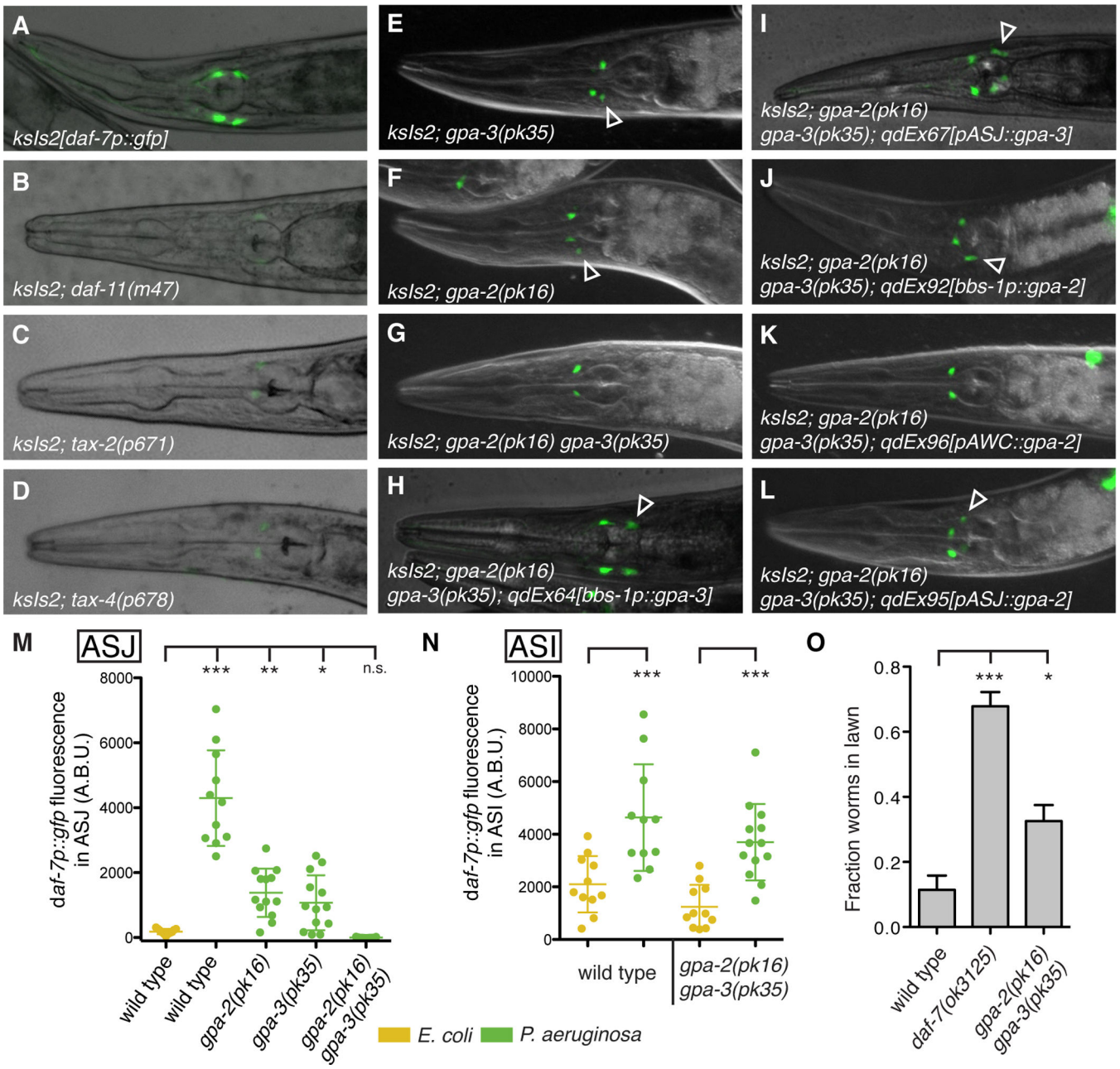

Figure 4. GPA-3 and GPA-2 function cell-autonomously in the ASJ neurons to activate *daf-7* expression in response to *P. aeruginosa*

(A–L) *daf-7p::gfp* expression on *P. aeruginosa* in various genetic backgrounds. Empty triangles indicate ASJ neurons. (M–N) Maximum fluorescence values of *daf-7p::gfp* in the ASJ (M) or ASI (N) neurons after 16 h exposure to indicated bacteria. (O) Lawn occupancy of animals on *P. aeruginosa* after 15 h. *** $P < 0.001$, ** $P < 0.01$, * $P < 0.05$ as determined by one-way ANOVA followed by Dunnett's Multiple Comparison Test. Error bars indicate standard deviation. See also Figure S4.

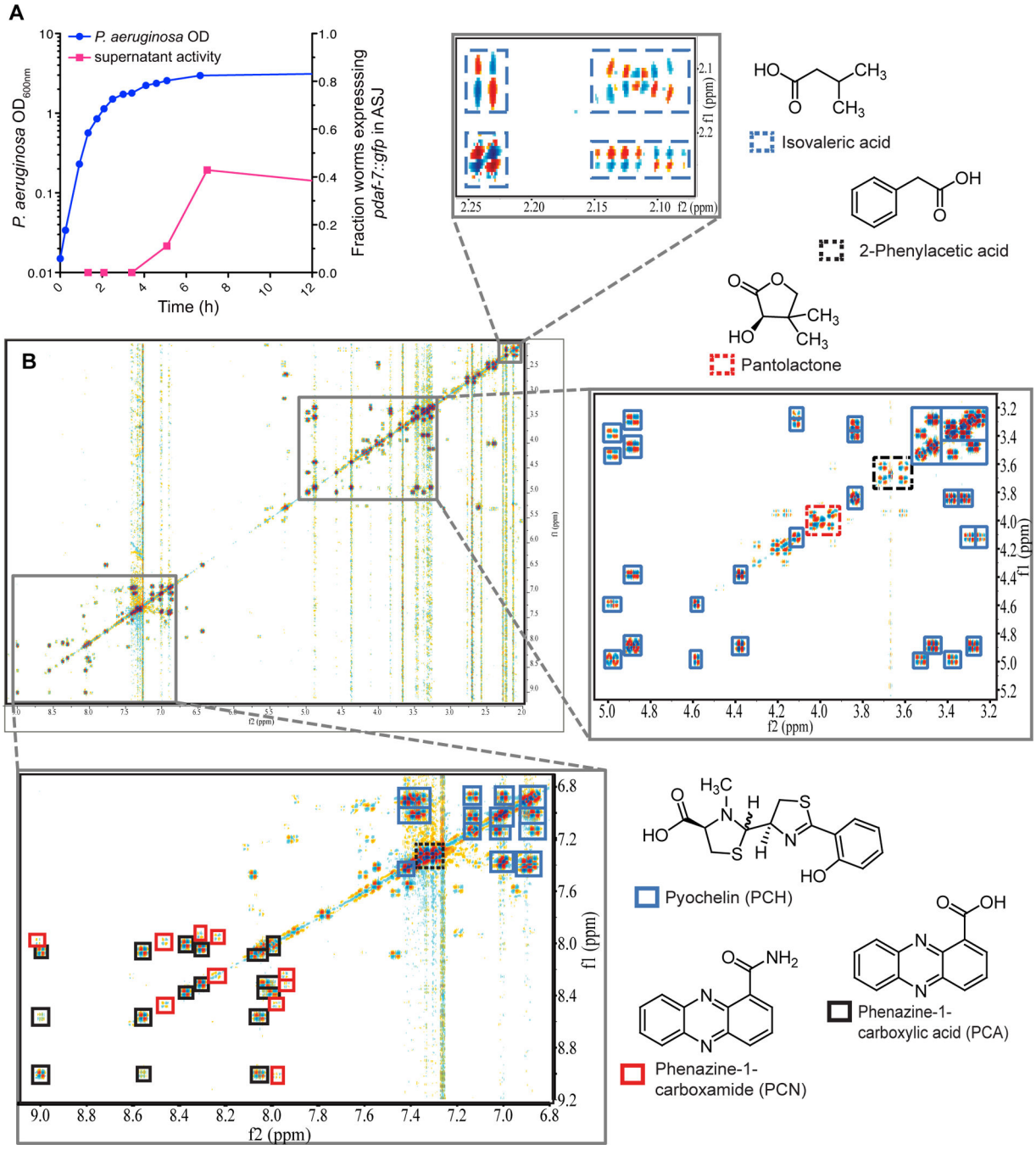

Figure 5. Supernatant from *P. aeruginosa* in stationary phase activates *daf-7* expression and contains secondary metabolites

(A) Growth curve of *P. aeruginosa* as measured by OD_{600nm} (blue circles) and activity of bacterial supernatant in inducing *daf-7p::gfp* expression in the ASJ neurons (magenta squares). (B) DQF-COSY spectrum of active metabolome fraction of *P. aeruginosa* media extract. Enlarged sections show cross-peaks of the most abundant metabolites present in this fraction. See also Figure S5.

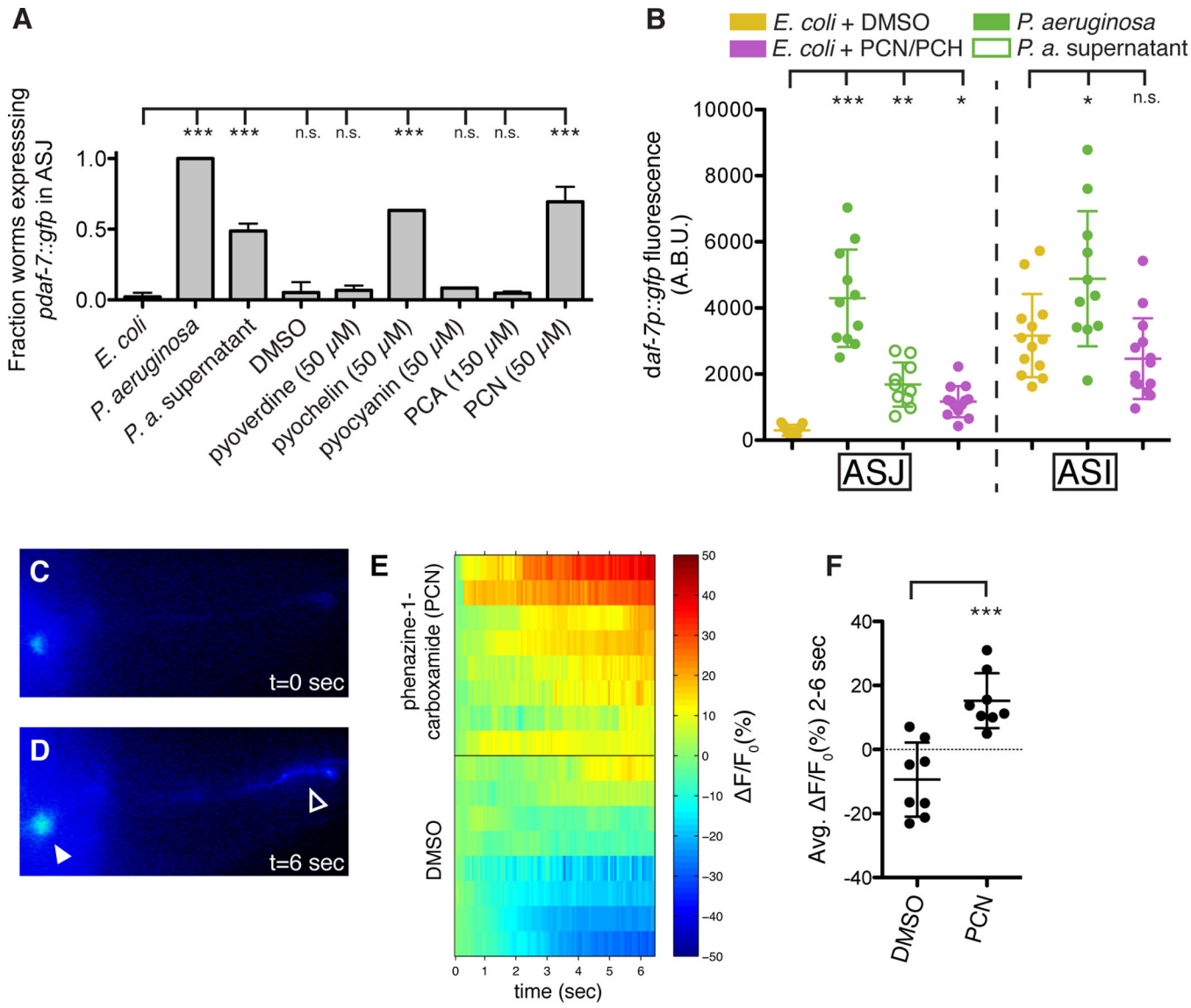

Figure 6. The ASJ neurons respond to *P. aeruginosa* secondary metabolites phenazine-1-carboxamide and pyochelin

(A–B) *daf-7p::gfp* expression in the ASJ or ASI neurons after 16 h exposure to *E. coli*, *P. aeruginosa*, or *E. coli* supplemented with indicated material. Data represent (A) the fraction of animals expressing *daf-7p::gfp* in ASJ above background or (B) the maximum fluorescence values of *daf-7p::gfp* in ASJ and ASI. All compounds were dissolved in DMSO. *** P < 0.001, ** P < 0.01, * P < 0.05 as determined by one-way ANOVA followed by Dunnett's Multiple Comparison Test. n.s. = not significant. Error bars indicate standard deviation. (C–D) GCaMP5 expression in the ASJ neurons immediately prior to (C) or following (D) addition of PCN. Filled triangle indicates the ASJ cell body and open triangle indicates the ASJ sensory projection. (E) GCaMP5 fluorescence changes in individual animals following the addition of PCN or DMSO at t = 0 seconds. (F) Average changes in GCaMP fluorescence in the 2–6 s following addition of either PCN or DMSO. *** P <

0.001 as determined by unpaired t-Test. Error bars indicate standard deviation. See also Figure S6.

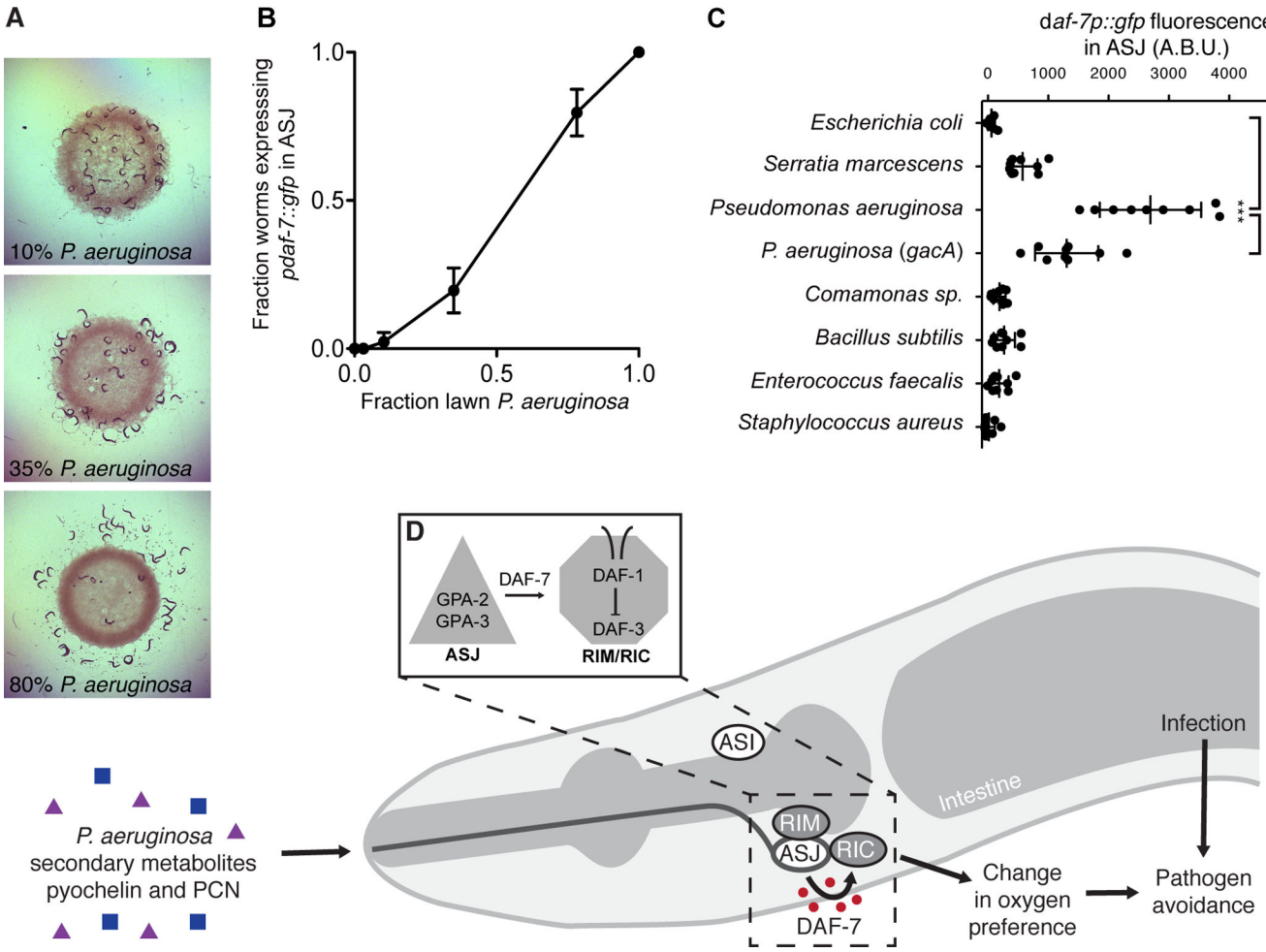

Figure 7. Microbial discrimination of *P. aeruginosa* activates *daf-7* transcription in the ASJ neurons and promotes avoidance behavior

(A) *C. elegans* after 16 h exposure to bacterial lawns consisting of *E. coli* OP50 and *P. aeruginosa* PA14. Fraction of bacteria that were *P. aeruginosa* when *daf-7p::gfp* was assayed is indicated. (B) Fraction of animals expressing *daf-7p::gfp* in the ASJ neurons after 16 h exposure to *E. coli*, *P. aeruginosa*, or mixtures of *E. coli* and *P. aeruginosa*. Error bars indicate standard deviation. (C) Maximum fluorescence values of *daf-7p::gfp* in ASJ neurons after 16 h exposure to indicated bacteria. *** $P < 0.001$ as determined by one-way ANOVA followed by Tukey's Multiple Comparison Test. Error bars indicate standard deviation. (D) In response to *P. aeruginosa* exposure, or *P. aeruginosa* metabolites phenazine-1-carboxamide (PCN) and pyochelin, *daf-7* expression is activated via G-protein alpha subunits GPA-3 and GPA-2 in the ASJ neurons. Secreted DAF-7 signals to the TGF-β receptor DAF-1 the adjacent RIM/RIC interneurons. DAF-7/TGF-β signaling acts to alter aerotaxis behavior and promote avoidance of pathogenic bacteria.